University of **Reading**

Spatial variations of N2O fluxes across the water‑air interface of mariculture ponds in a subtropical estuary in southeast China

Article

Accepted Version

Yang, P., Wang, D., Lai, D. Y. F., Zhang, Y., Guo, Q., Tan, L., Yang, H. ORCID: https://orcid.org/0000-0001-9940-8273, Tong, C. and Li, X. (2020) Spatial variations of N2O fluxes across the water‑air interface of mariculture ponds in a subtropical estuary in southeast China. Journal of Geophysical Research: Biogeosciences, 125 (9). e2019JG005605. ISSN 2169-8961 doi: https://doi.org/10.1029/2019JG005605 Available at http://centaur.reading.ac.uk/95944/

It is advisable to refer to the publisher's version if you intend to cite from the work. See Guidance on citing.

www.reading.ac.uk/centaur

CentAUR

Central Archive at the University of Reading

Reading's research outputs online

Spatial Variations of N_2O Fluxes Across the Water-Air Interface of Mariculture Ponds in a Subtropical Estuary in Southeast China

Ping Yang[1,2] , Dongqi Wang[3] , Derrick Y. F. Lai[4] , Yifei Zhang[1,2], Qianqian Guo[1,2], Lishan Tan[1,2,3], Hong Yang[5,6,7] , Chuan Tong[1,2] , and Xiaofei Li[1,2]

1 Key Laboratory of Humid Subtropical Eco-geographical Process of Ministry of Education, Fujian Normal University, Fuzhou, China,

2 School of Geographical Sciences, Fujian Normal University, Fuzhou, China,

3 School of Geographical Sciences, East China Normal University, Shanghai, China,

4 Department of Geography and Resource Management and Centre for Environmental Policy and Resource Management, The Chinese University of Hong Kong, Hong Kong,

5 Collaborative Innovation Center of Atmospheric Environment and Equipment Technology, Jiangsu Key Laboratory of Atmospheric Environment Monitoring and Pollution Control (AEMPC), School of Environmental Science and Engineering, Nanjing University of Information Science and Technology, Nanjing, China,

6 College of Environmental Science and Engineering, Fujian Normal University, Fuzhou, China, 7Department of Geography and Environmental Science, University of Reading, Reading, UK

Abstract

While aquaculture ponds are potentially important sources of atmospheric N_2O, the magnitude and variability of N_2O concentrations and fluxes both within and across the ponds remain poorly understood. In this study, we examined the small-scale spatial variations of dissolved N_2O concentrations in water and N_2O fluxes across the water-air interface from three mariculture ponds in a subtropical estuary in southeast China. Our results showed that the dissolved concentrations and diffusive fluxes of N_2O in the shrimp ponds ranged between 2.3–19.2 nM and 16.4–589.7 nmol m^{-2} hr^{-1}, respectively, over the culture period. Significant variations of N_2O concentrations and fluxes were observed within the ponds, with higher values being observed in the aeration area that could be attributed to the high rates of nitrification in the water column, as well as sediment N_2O production and diffusive flux into the overlying water. Also, N_2O concentrations and fluxes varied significantly among the three ponds as a result of the difference in N-NO_3^- and N-NH_4^+ concentrations in the water column. The large fine-scale spatial variations of N_2O concentrations and fluxes observed in our aquaculture ponds suggested that management practices such as aeration and bait feeding could largely affect the extent that aquaculture activities have on N_2O emissions and climate change through their influence on the physicochemical environment (e.g., oxygen and N-NH_4^+ concentrations) of the ponds.

1 Introduction

Nitrous oxide (N_2O) is a long-lived potent greenhouse gas (GHG) with a global warming potential that is approximately 300 times higher than that of carbon dioxide (CO_2) over a 100-year time scale (Intergovernmental Panel on Climate Change [IPCC], 2013). It is also considered as the single most important ozone-depleting gas (Ravishankara et al., 2009). Since the Industrial Revolution, the global mean atmospheric N_2O concentration had increased steadily by approximately 121% to 331.1 ± 0.1 ppbv in 2018 (World Meteorological Organization [WMO], 2019). Quantifying the magnitude of and the effects of human activities on N_2O emissions from various ecosystems has thus become a top priority for improving the estimation of global N_2O budgets.

In general, N_2O is mainly produced either as an intermediate product during the stepwise reduction of NO_3^- (by heterotrophic denitrification), as a by-product during the autotrophic oxidation of ammonia and hydroxylamine, or as a product of nitrifier denitrification during the reduction of nitrite under anoxic conditions (Butterbach-Bahl et al., 2013; Dalsgaard et al., 2014; Sutka et al., 2006). Nitrogen and oxygen availability has been reported to be an important factor controlling the processes of N_2O production (e.g., Beaulieu et al., 2011; Dalsgaard et al., 2014; Gruber & Galloway, 2008; Murray et al., 2015). Due to the vast application of N fertilizers in farmlands, agricultural activity is widely considered to be one of primary anthropogenic sources of N_2O (S. Liu et al., 2017; McCarl & Schneider, 2001; Wu et al., 2018), accounting for about 60% of the global anthropogenic N_2O emission (IPCC, 2013). As an indispensable part of global agriculture, the aquaculture industry has a wide distribution around the world, particularly in the developing countries (Food and Agriculture Organization [FAO], 2017). The emission of N_2O from aquaculture systems has received increasing attention recently (Z. Hu et al., 2012, 2014; Liu et al., 2016; Paudel et al., 2015; P. Yang, Bastviken, et al., 2017; Yogev et al., 2018). The total N_2O-N emission from the world's aquaculture systems was estimated to be to 90 Gg in 2009, accounting for approximately 0.5% of the global N_2O-N emission (Williams & Crutzen, 2010). The contribution of aquaculture systems to the annual anthropogenic N_2O-N emission is expected to increase to about 6% by 2030, assuming a 7–10% annual growth rate of the industry (Z. Hu et al., 2012). However, these estimates are highly uncertain since the contribution of N_2O emissions from coastal mariculture ponds is largely unknown. Mariculture is an important component of global aquaculture that is commonly practiced in the coastal areas (FAO, 2017). According to the statistical records of the FAO, the total surface area of global mariculture ponds is around 23,332 km^2 (Verdegem & Bosma, 2009). In spite of the importance of quantifying N_2O fluxes from mariculture systems for constructing global N_2O budget and national emission inventories, there is a paucity of studies examining the

magnitude and controlling factors of N_2O exchange across the water-air interface of mariculture ponds.

The mariculture industry in China is the largest in the world (Gu et al., 2017), comprising over 17% of the global mariculture volume and approximately 33% of the total production value in 2014. Aquaculture is the most dominant method of shrimp production in the subtropical estuarine zones of China (P. Yang, Bastviken, et al., 2017). Mariculture shrimp ponds are generally semiartificial ecosystems that are heavily managed by practices such as stocking, feeding, harvesting, and aeration (Chen et al., 2016; P. Yang et al., 2018). These ponds are inherently heterogeneous over multiple spatiotemporal scales as a result of differences in topographic features, environmental conditions, and management actions (P. Yang et al., 2019). However, the fine-scale spatial variations of N_2O fluxes both within and between ponds and their temporal changes remain poorly characterized. Detailed *in situ* measurements of N_2O dynamics across various spatial and temporal scales are crucial for improving our understanding of GHG fluxes in ponds and developing more accurate approaches for upscaling aquaculture N_2O emissions from point measurements to the whole pond or even regional scale.

In this research, the small-scale spatial variations of dissolved N_2O concentration and flux across the water-air interface of three shrimp ponds in a subtropical estuary in southeast China were investigated to shed light on the N_2O dynamics in the aquaculture ponds and its implications for flux upscaling to the regional scale. The specific objectives of this study were to (1) characterize the spatiotemporal variations of N_2O concentrations and fluxes within and between the mariculture ponds; and (2) examine the main factors governing the differences in pond N_2O concentrations and fluxes across space and time.

2 Materials and Methods

2.1 Study Area

Our field measurements were conducted in the mariculture ponds in the Shanyutan wetland in the Min River Estuary in southeast China (Figure 1; P. Yang et al., 2019), which covered a total area of approximately 234 ha (P. Yang, Lai, et al., 2017). The study area was influenced by a subtropical monsoonal climate, with annual mean temperature and precipitation of 19.60°C and 1,350 mm, respectively (Tong et al., 2010). The native *Cyperus malaccensis* (shichito matgrass), *Phragmites australis* (common reed), and the invasive *Spartina alterniflora* (smooth cordgrass) were the dominant vegetation species in the area. The shrimp ponds were created by removing the original marsh vegetation (P. Yang, Bastviken, et al., 2017). The wetland was influenced by semidiurnal tides, with the surface soil being submerged during the two flood tide periods (Tong et al., 2010).

2.2 Shrimp Pond System and Operation

Three shrimp (*Litopenaeus vannamei*) ponds were randomly selected within a radius of 200 m in our study area, with the geographical coordinates of Pond I, Pond II, and Pond III being 26°01′48″N and 119°37′37″E, 26°01′44″N and 119°37′48″E, and 26°01′41″N and 119°37′52″E, respectively. Shrimp production was generally carried out in the coastal shrimp ponds during the period from June to November. Before shrimp production, the ponds were filled with seawater pumped from the adjacent estuary (P. Yang et al., 2018). During the culture period, the ponds had no drainage or addition of water, except occasional introduction of freshwater by rainfall. The shrimps were regularly fed with commercial pellets (Hangsheng and Tianma Chia Tai Feed Co., Ltd., Fuzhou, China) twice a day (07:00 a.m. and 16:00 p.m., local standard time) manually from a boat. The feed dosage decreased in the following order: July and August > September and October > June and November. In order to increase the oxygen level in water, three to five 1,500-W paddlewheel aerators were operated in each pond four times a day (00:00–03:00, 07:00–09:00, 12:00–14:00, and 18:00–20:00). According to the spatial variations of microtopographic features, water depth, and management practices, the shrimp ponds were divided into three different zones, namely, Zone N, which was a nearshore area with sparse submerged vegetation, Zone F, which was a deepwater area used for feeding, and Zone A, which was a shallow-water area subjected to aeration activities (Figure 1c). Please refer to Zhang et al. (2019) and P. Yang et al. (2019) for more details about the overall setup and the three spatial zones of these shrimp ponds. Details about the management practices in these shrimp ponds can be found in P. Yang, Lai, et al. (2017) and P. Yang et al. (2018).

2.3 Collection and Analysis of Surface Water Samples

Six sampling campaigns were carried out during the aeration period of 12:00–14:00 at monthly intervals during the entire aquaculture period between June and November 2017 according to the timing of the main management practices. Since no clear difference in N_2O concentration was found between the surface and bottom waters in the shallow shrimp ponds (with depths ranging from 1.4–1.8 m) (unpublished data), only the surface water samples were collected at 0- to 20-cm depth for analysis. In each sampling campaign, three transects that ran across the three zones were selected in each pond for determining the N_2O concentration and saturation in water (Figure 1c). Water samples were collected at 20-cm depth using a custom-made sampler equipped with a rubber cork, flushed into the 55-ml preweighted serum glass bottles for two to three times, and then completely filled to the top of the bottles. About 0.2 ml of saturated $HgCl_2$ solution was added to the bottles for inhibiting bacterial activity (Borges et al., 2018), and the glass bottles were then immediately sealed with an open-topped screw cap equipped with a halobutyl rubber septum to exclude any air

bubbles (Borges et al., 2018; X. F. Wang, He, et al., 2017; Xiao et al., 2019). The water samples were subsequently stored in an ice-packed cooler, transported back to the laboratory, and analyzed within 48 hr. N_2O concentration was measured using a gas chromatograph (Shimadzu GC-2014, Kyoto, Japan) equipped with an electron capture detector, after calibration with three N_2O gas standards with concentrations of 0.3, 0.4, and 1.0 ppm, respectively. The N_2O detection limit was 0.02 ppm, and the measurement reproducibility was ±4.5% in 24 hr. The dissolved N_2O concentrations in water were determined based on the headspace equilibration method and Henry's law constant. Dissolved N_2O concentration (nmol N_2O L^{-1}) and saturation (%) in water were calculated following B. Hu et al. (2018).

2.4 N_2O Flux Calculation

The diffusive N_2O fluxes (F_{W-A}, nmol m^{-2} hr^{-1}) across the water-air interface were calculated based on the gas transfer coefficient method following Equation 1 (Jahne et al., 1987; MacIntyre et al., 1995; Xiao et al., 2017):

$$F_{W-A} = k \ \times \ \Delta C,$$

(1)

where k was the gas exchange velocity (cm hr^{-1}) and ΔC was the difference in N_2O concentration between the air and water. The k value was influenced by wind speed and normalized to a Schmidt number of 600 (Jahne et al., 1987; MacIntyre et al., 1995; Xiao et al., 2017). Wind speed was measured and recorded by an automatic weather station at the Min River Estuary Ecological Station in the Shanyutan Wetland. The k values from Cole and Caraco (1998) were applied in this research as their field environment was similar to ours.

2.5 Measurement of Ancillary Data

The *in situ* water temperature and pH at 20-cm depth were measured with a portable pH/mV/Temperature meter system (IQ150, IQ Scientific Instruments, USA). Dissolved oxygen (DO) and salinity were determined by a DO meter (550A YSI, USA) and a salinity meter (Eutech Instruments-Salt6, USA), respectively. Surface water samples (20-cm depth) were collected from the three zones using an organic glass hydrophore, transferred into 150-ml polyethylene bottles, immediately transported back to the laboratory in an ice-packed cooler, stored at 4°C, and analyzed within 1 week.

In the laboratory, approximately 100 ml of water sample was filtered through a 0.45-μm filter (Biotrans™ nylon membranes) and analyzed for inorganic N (N-NH_4^+ and N-NO_3^-) using a flow injection analyzer (Skalar Analytical SAN++, Netherlands). Meteorological data including air temperature, atmospheric pressure, wind speed, and precipitation were obtained from the automatic weather station.

2.6 Statistical Analyses

Data were presented as means ±1 standard error. Three-way analysis of variance (ANOVA) was performed to analyze the effects of zone, pond, and month and their interactions on N_2O concentrations and fluxes across the water-air interface in the mariculture ponds. Stepwise regression analysis was conducted to determine the most important factors governing N_2O concentrations and fluxes across the water-air interface in the shrimp ponds. Spearman correlation analysis was performed to examine the relationships between N_2O concentration (or N_2O flux) and various environmental variables. All statistical analyses were carried out using the SPSS statistical software package (Version 17.0, SPSS Inc., USA), and results were considered significant at the 0.05 level.

3 Results

3.1 Spatial Variations of Water Physicochemical Parameters

The spatial variations of water physicochemical variables within and among the ponds during the aquaculture period are shown in Figures 2 and 3. There were no significant differences in mean temperature, salinity, pH, and $N-NO_x^-$ among the three sampling zones ($p > 0.05$; Figure 2 and Table S1 in the supporting information). However, there were significant differences in mean DO (Figures 2b and S1) and $N-NH_4^+$ (Figures 2f and S2) among the three zones of the ponds ($p < 0.01$; Table S1). Overall, the means of DO and $N-NH_4^+$ were significantly higher at Zone A than those at Zones F and N ($p < 0.01$).

Most of the physicochemical properties of water, including water temperature, DO, and pH, were similar among the three ponds ($p > 0.05$; Figure 3 and Table S1; Zhang et al., 2019), except for salinity, $N-NO_x^-$ and $N-NH_4^+$ ($p < 0.01$; Figure 3 and Table S1). Across all sampling campaigns, $N-NO_x^-$ concentrations varied over the range of 24–350, 21–110, and 23–140 µg L^{-1} in Ponds I, II and III, respectively, while $N-NH_4^+$ concentrations varied over the range of 0.1–0.7, 0.1–1.4, and 0.1–0.7 mg L^{-1}, respectively, in the three ponds. Overall, the mean $N-NO_x^-$ and $N-NH_4^+$ concentrations decreased significantly among the three ponds in the order: Pond II > Pond III > Pond I ($p < 0.05$; Figures 3c and 3d and Table S1).

3.2 Spatial Variations of N_2O Concentrations and Fluxes Within Ponds

Across all sampling campaigns, dissolved N_2O concentrations in Zones N, F, and A varied in the range of 4.65–20.31, 4.29–19.72, and 5.18–23.09 nmol L^{-1} (Figure 4), respectively, which corresponded to N_2O saturations of 98–314%, 89–305%, and 108–358%, respectively. Average N_2O concentration decreased significantly in the following order: Zone A (10.64 ± 0.58 nmol L^{-1}) > Zone F (9.20 ± 0.50 nmol L^{-1}) > Zone N (8.55 ± 0.48 nmol L^{-1})

($p < 0.001$; Table S2 and Figure S4a). The mean N_2O saturations in Zones N, F, and A were $157 \pm 6.1\%$, $144 \pm 5.9\%$, and $180 \pm 7.6\%$, respectively.

There were considerable spatial variations of N_2O diffusion fluxes across the three zones of the ponds over the study period ($p < 0.001$; Table S2 and Figures 5a and S5). N_2O fluxes in Zones N, F, and A varied over the range of 10.75–712.06, 0.24–666.80, and 25.06–948.27 nmol m^{-2} hr^{-1} (Figure S5), respectively. Over the whole study period, Zone A exhibited a significantly higher mean N_2O emission (231.56 ± 28.34 nmol m^{-2} hr^{-1}) than Zones N (156.16 ± 20.11 nmol m^{-2} hr^{-1}) and F (119.52 ± 18.13 nmol m^{-2} hr^{-1}) ($p < 0.001$; Table S2 and Figure 5a).

3.3 Spatial Variations of N_2O Concentrations and Fluxes Among Ponds

Across all sampling dates and zones, the N_2O concentrations in Pond I, II, and III varied over the range of 4.85–14.42, 5.09–23.09, and 4.23–15.45 nmol L^{-1} (Figure 4), respectively. Average N_2O concentrations differed significantly among the three ponds in the following descending order: Pond II (11.11 ± 0.69 nmol L^{-1}) > Pond III (8.69 ± 0.42 nmol L^{-1}) > Pond I (8.58 ± 0.35 nmol L^{-1}) ($p < 0.05$; Table S2 and Figure S4b). N_2O saturations in water varied from 104% to 310%, suggesting that the ponds were consistent N_2O sources.

N_2O fluxes in Ponds I, II, and III varied over the ranges of 5.22–477.39, 6.63–948.27, and 0.24–387.51 nmol m^{-2} hr^{-1}, respectively (Figure S5). Overall, the average N_2O flux differed significantly among the three ponds in the following descending order: Pond II (247.65 ± 33.25 nmol m^{-2} hr^{-1}) > Pond I (134.54 ± 14.28 nmol m^{-2} hr^{-1}) > Pond III (128.70 ± 13.06 nmol m^{-2} hr^{-1}) ($p < 0.01$; Figure 5b and Table S2).

3.4 Relationship Between N_2O Concentrations/Fluxes and Environmental Variables

Significant correlations were found between N_2O concentrations (or fluxes) and DO concentrations across all three zones and ponds during each sampling campaign ($p < 0.01$; Figures S6 and S7). The mean N_2O concentrations (or fluxes) were also positively correlated with the mean concentrations of $N\text{-}NO_x^-$ ($p < 0.01$; Figures S8 and S9) and $N\text{-}NH_4^+$ concentrations ($p < 0.01$; Figures S10 and S11) in water across all zones and ponds on each sampling campaign. The Spearman correlation coefficients between the surface water N_2O concentrations (or fluxes) and environmental variables at the mariculture ponds during the aquaculture period are shown in Table S3.

4 Discussion

4.1 Spatial Variations in N_2O Emission Fluxes Between Ponds

Nitrification and denitrification are the most important microbial processes influencing N_2O production in aquatic systems (Beaulieu et al., 2011; D. Q. Wang, Tan, et al., 2015; Wenk et al., 2016) and are governed by various biotic and abiotic factors. Nitrogen (N) substrate and oxygen supply are some key factors controlling the N_2O production processes (Dalsgaard et al., 2014; Liang et al., 2019; Massara et al., 2018; Yu et al., 2013). In general, a high nitrite ($N-NO_2^-$) concentration can stimulate nitrifier denitrification, which is largely responsible for N_2O production in sediments (Murray et al., 2015), while a high $N-NH_4^+$ concentration can promote N_2O production through hydroxylamine oxidation either in the sediment or the water column (Barnes & Upstill-Goddard, 2011; J. N. Wang, Chen, et al., 2015). Meanwhile, heterotrophic denitrification, an important pathway of N_2O production in sediments, is favored under low DO and high nitrate ($N-NO_3^-$) concentrations (Dalsgaard et al., 2014; Xia et al., 2018). As a result, large spatial variations of N_2O fluxes have been reported in various aquatic ecosystems, including rivers (B. Hu et al., 2018; Rajkumar et al., 2008; Tan, 2014), reservoirs (Guérin et al., 2008; Musenze et al., 2014; X. F. Wang, He, et al., 2017), and lakes (Y. S. Liu et al., 2011; H. J. Wang et al., 2006; S. L. Wang et al., 2009) with various N loading and oxygen level. Notably, the availability of N substrates has been found to play an important role in governing the spatial variability of N_2O fluxes within lakes in the subtropical and Antarctic regions (Y. S. Liu et al., 2011; H. J. Wang et al., 2006; S. L. Wang et al., 2009). Yet, to the best of our knowledge, such information is rare for shallow water ponds, especially those created for mariculture activities.

One interesting finding of this study was that the average N_2O fluxes differed significantly among the three ponds (Table S2), with the largest value being observed in Pond II (Figures 5b and S5). This spatial variability of N_2O flux could be primarily ascribed to the differences in the physicochemical parameters of sediment and water. Among all the variables investigated in this study, only water $N-NO_x^-$ and $N-NH_4^+$ concentrations differed significantly among the ponds ($p < 0.01$; Figure 3 and Table S1). The average water $N-NO_x^-$ concentration at Pond II was 1.3–3.9 times and 1.2–1.9 times higher than that at Ponds I and III, respectively. Similarly, the mean $N-NH_4^+$ concentration at Pond II was 1.2–2.1 times and 1.1–4.2 times higher than that at Ponds I and III, respectively. The significantly higher concentrations of $N-NO_x^-$ and $N-NH_4^+$ observed in Pond II were likely related to the massive shrimp mortality in this pond during the later part of the culture period, which reduced the efficiency of feed utilization and contributed to the accumulation of nutrients in the water column. The larger supply of N substrates played an important role in sustaining a larger N_2O efflux at Pond II, as compared to Ponds I and III. This was further confirmed by the

significant correlation observed between N_2O concentrations (fluxes) with water $N\text{-}NO_x^-$ and $N\text{-}NH_4^+$ concentrations ($p < 0.01$; Figures S8–S11).

4.2 Aeration Zones as N_2O Emission Hotspots Within Ponds

Mariculture ponds are often aerated on a daily basis to help increase oxygen supply to pond water. Previous studies have found that a large wind speed can increase gas transfer velocity across the water-air interface and thus the rate of GHG efflux (Bates et al., 1998; B. Hu et al., 2018; Musenze et al., 2014; Nemoto et al., 2009). The results of our plot-scale *in situ* experiments showed that considerable small-scale spatial variations of N_2O flux existed within mariculture ponds (Table S2), with larger flux being obtained at Zone A across all sampling dates (Figures 5a and S5). Importantly, our results suggested that the whole-pond mean N_2O fluxes could be underestimated if measurements were only done in the nearshore and feeding areas without considering the aeration zone.

Aeration activities can induce the disturbance of pond water and subsequently increase the gas transfer velocity across the water-air interface for diffusive transport at Zone A considerably. In addition, aeration activities can increase the DO level, which in turn can govern the N_2O production rates by stimulating microbial nitrification (Y. S. Liu et al., 2011; Rosamond et al., 2012). Previous studies have reported that the $N\text{-}NH_4^+$ can be oxidized to $N\text{-}NO_3^-$ via nitrifier nitrification, with N_2O being a byproduct, under a high DO level (Beaulieu et al., 2015; Liang et al., 2019; Maavara et al., 2019; Rosamond et al., 2011). As a result, the high concentrations of $N\text{-}NH_4^+$ and DO are considered to be favorable for N_2O production associated with nitrification in aerobic aquatic systems (Cheng et al., 2019; Rosamond et al., 2012; Sturm et al., 2014; Whitfield et al., 2011). Culture aquatic animals, such as shrimps in our study, are generally fed several times a day (Chen et al., 2016; P. Yang et al., 2018). The mineralization of residual feeds and feces can produce a large amount of dissolved $N\text{-}NH_4^+$ in the mariculture ponds (Figure 2e). Strong turbulence caused by aeration activities might have transported $N\text{-}NH_4^+$ rich water at the pond bottom to the pond surface, where the high DO level would support a higher nitrifier nitrification and hence a high N_2O production in the water column at Zone A. In our study ponds, there were significant and positive relationships between N_2O concentrations (fluxes) and (1) water DO concentrations ($p < 0.01$; Figures S6 and S7) and (2) $N\text{-}NH_4^+$ concentrations ($p < 0.01$; Figures S10 and S11), which supported the hypothesis that nitrification was one important pathway of N_2O production in the pond water.

Previous studies in marine systems have shown that the oxic-anoxic interface is a site of intense N_2O flux (Arevalo-Martinez et al., 2015; Cohen & Gordon, 1978; Goreau et al., 1980; Ji et al., 2015). At this critically low, but nonzero, oxygen concentration at the oxic-anoxic interface, N_2O production from both nitrification and denitrification could be enhanced while

N$_2$O consumption would be inhibited, resulting in an overall peak N$_2$O emission (Ji et al., 2015). Similar results have been found in aquaculture ponds, with an enhanced N$_2$O production under low DO conditions (Z. Hu et al., 2012, 2013; Liu et al., 2016). Even in a fully oxic water column, oxygen can be rapidly depleted in benthic sediments (Yu et al., 2013), leading to the dominance of anaerobic conditions and thus denitrification process in the subsurface sediment layers (Hinshaw & Dahlgren, 2013; Liang et al., 2019; Xia et al., 2018). Meanwhile, nitrification could cooccur at the oxic-anoxic interface of pond surface sediments. Therefore, the high N$_2$O emissions obtained at Zone A in the present study could at least in part be linked to the high N$_2$O production from both nitrification and dentification under low-O$_2$ conditions at the sediment-water interface. Once N$_2$O was produced in the sediments, it could be transported readily into the overlying water of these shallow ponds through diffusion and aeration-induced mechanical mixing. Further studies using controlled experiments should be carried out to test the above hypothesis.

4.3 Mariculture Ponds as an Important N$_2$O Emission Source

Based on the gas transfer coefficient method, the mean diffusion N$_2$O flux from the whole pond was estimated to be 169.1 nmol m^{-2} hr^{-1}. Notably, the mean N$_2$O emission from our ponds during the aquaculture period was markedly lower than the average of 721 nmol m^{-2} hr^{-1} found in the *Cyperus malaccensis* marsh in an adjacent estuary during the summer and autumn periods (X. M. Wang et al., 2018). Our results suggested that the conversion of brackish marsh ecosystem to shrimp ponds could reduce N$_2$O emissions during the aquaculture period. This was in agreement with the results of S. W. Liu et al. (2016), Wu et al. (2018), and P. Yang, Bastviken, et al. (2017), in which N$_2$O fluxes reduced following the conversion of rice paddies or coastal marshes to aquaculture ponds.

The magnitude of N$_2$O flux in our ponds was lower than those observed in rivers in the temperate and tropical regions (B. Hu et al., 2018; Laini et al., 2011; Silvennoinen et al., 2008; Tan, 2014), as well as some reservoirs (Descloux et al., 2017; Guérin et al., 2008; X. F. Wang, He, et al., 2017) and lakes in the temperate and subtropical regions (Y. S. Liu et al., 2011; H. J. Wang et al., 2006; H. X. Wang, Zhang, et al., 2017) (Table 1). However, the N$_2$O fluxes in our ponds were substantially higher than those in the majority of freshwater aquaculture ponds in China (Li et al., 2019; S. W. Liu et al., 2016; Wu et al., 2018) and Vietnam (Paudel et al., 2015) (Table 1). Furthermore, our observed N$_2$O fluxes were more than 13-fold higher than those observed in the reservoirs in Southeast Queensland in Australia (Musenze et al., 2014), substantially higher than those reported in a freshwater lake in Poyang Lake in China (H. X. Wang, Zhang, et al., 2017), and several lakes in Antarctica (Y. S. Liu et al., 2011) (Table 1). The mean N$_2$O diffusive flux from our mariculture ponds was also comparable to that from the coastal Lake Nakaumi in Japan (Hirota et al., 2007)

(Table 1). Our results highlighted that mariculture shrimp ponds are important sources of atmospheric N_2O that are often overlooked in assessing the regional and global N_2O budgets.

4.4 Implications of the Spatiotemporal Variations of N_2O Flux

Previous studies examining the spatial and temporal variations of GHG emissions from reservoirs and lakes have suggested that the lack of flux measurements at a high spatiotemporal resolution across and within aquatic ecosystems has contributed to the large uncertainties of regional to global estimates of GHG budgets (Musenze et al., 2014; Natchimuthu et al., 2017; H. Yang & Flower, 2012; H. Yang et al., 2011). The paucity of *in situ* field measurements of gas fluxes at small-scale spatial resolution is also a possible cause for the biases in the estimation of large-scale GHG emissions. Here, this study made the first attempt to characterize the small-scale spatial variations of N_2O fluxes from the estuarine mariculture ponds over the culture period. Overall, our results showed that the estuarine mariculture ponds were important atmospheric N_2O sources with large spatial variations both within and among the ponds. The significantly higher N_2O fluxes in the aeration area (Zone A) suggested that previous studies that only measured fluxes in the nearshore area (Zone N) could have largely underestimated the magnitude of N_2O emissions from aquaculture ponds (Ma et al., 2018; Wu et al., 2018; P. Yang, Bastviken, et al., 2017). Accurate upscaling of N_2O fluxes measured by chambers to the whole-pond or even larger spatial scales requires a good coverage of a sufficient number of strategically located sites with representative N_2O flux values. The significant within-pond differences in mean N_2O fluxes implied that the extrapolation of N_2O emissions obtained from scattered spots in the ponds to the regional or global scale should be done cautiously. Meanwhile, the significant temporal variations of N_2O fluxes (Figure 5) suggested that the extrapolation of fluxes based on field measurements made in a single month to seasonal or annual scales could also lead to considerable biases. Therefore, future studies should conduct flux measurements from as many sites as practicable over multiple months in order to produce more reliable estimates of N_2O flux and enhance our understanding of N_2O dynamics in mariculture ponds.

4.5 Limitations and Future Outlook

There was a certain degree of uncertainty associated with the N_2O flux estimates derived in our work, similar to other previous studies that adopted the wind-based gas transfer method. The N_2O flux in our study was estimated based on the gas transfer velocity coefficient (k_x) and the N_2O concentration gradient between the surface water and the atmosphere. The k_x values were derived from some empirical wind-based models only without direct field measurements. Moreover, samples for the determination of dissolved N_2O concentrations were taken at Zone A only during the aeration period but not the pre-aeration and postaeration periods. Hence, there might be bias in our estimated fluxes without taking into

full account the temporal variability of k_x and N_2O concentration before, during, and after aeration in the ponds. Given this uncertainty, future research should be done to provide site-specific quantification of k_x values as well as assess the effect of aeration on k_x and dissolved N_2O concentration in aquaculture ponds.

In addition, the findings of this study were limited by other several factors, which should be carefully considered in future studies. First, our field measurement of N_2O concentrations and fluxes was performed in one estuary during the mariculture period (from June to November) only, but not the entire year. The limited number of estuarine sites might constrain the spatial representativeness of our data at the regional and national scales. To obtain a more accurate estimate of N_2O fluxes in mariculture ponds, long-term observations at multiple estuaries in different regions should further be made. Second, this study did not quantify the diel variations of N_2O concentrations and fluxes, which might introduce some uncertainties to our N_2O estimates. Since diurnal variations of GHG emissions have been reported in lakes (e.g., Xing et al., 2004), such fine-scale changes in N_2O fluxes over time might also occur in our mariculture ponds. Third, our mariculture ponds and many other waterbodies in the southeastern coast of China are often affected by multiple typhoons every year. Considering the strong effect of wind speed on the k values across the water-air interface (Lévy et al., 2012; Natchimuthu et al., 2016; Ye et al., 2017), previous studies have found that the typhoon-associated strong winds can enhance GHG fluxes in aquatic ecosystems (Bates et al., 1998; Crosswell et al., 2014; Ye et al., 2017). Lastly, since the wind-based gas transfer method may not be able to capture the full effect of aeration systems on pond N_2O fluxes owing to the creation of significant turbulence, future studies should be conducted employing other alternative measurement techniques (e.g., eddy covariance) to quantify the water-air exchange of N_2O in mariculture ponds during the human-induced aeration of water bodies.

5 Conclusions

This study analyzed the spatial variations of N_2O concentrations in the water column and N_2O flux across the water-air interface, both within and among the mariculture ponds in the Shanyutan Wetland of Min River Estuary in southeast China. Our results showed that the estuarine mariculture ponds were an important atmospheric N_2O source with large spatial variations. Pond aeration and N substrate supply played important roles in governing the fine-scale spatial variations of N_2O fluxes. Our N_2O flux measurements made at the aeration, feeding, and nearshore areas in multiple shrimp ponds generated new insights into the spatial variability of N_2O fluxes and indicated the potential bias of whole-pond flux estimates determined based on field data from a single site without considering the emission hotspots. There were also large spatial variations of N_2O emission among individual ponds over the study period. The significant inter-pond differences further indicated the high uncertainty of

extrapolating GHG fluxes determined from a few ponds to the regional scale. Overall, our results highlighted the importance and urgency of making flux measurements from as many sites and ponds as practicable over a long time period in order to reduce the uncertainty and improve the confidence of upscaling N_2O emission data collected in the field to a larger scale.

Acknowledgments

References

Arevalo-Martinez, D. L., Kock, A., Loscher, C. R., Schmitz, R. A., & Bange, H. W. (2015). Massive nitrous oxide emissions from the tropical South Pacific Ocean. Nature Geoscience, 8(7), 530– 533. https://doi.org/10.1038/ngeo2469

Barnes, J., & Upstill-Goddard, R. C. (2011). N_2O seasonal distributions and air-sea exchange in UK estuaries: Implications for the tropospheric N_2O source from European coastal waters. Journal of Geophysical Research, 116, G01006. https://doi.org/10.1029/2009JG001156

Bates, N. R., Knap, A. H., & Michaels, A. F. (1998). Contribution of hurricanes to local and global estimates of air-sea exchange of CO_2. Nature, 395(6697), 58– 61. https://doi.org/10.1038/25703

Beaulieu, J. J., Nietch, C. T., & Young, J. L. (2015). Controls on nitrous oxide production and consumption in reservoirs of the Ohio River Basin. Journal of Geophysical Research: Biogeosciences, 120, 1995– 2010. https://doi.org/10.1002/2015jg002941

Beaulieu, J. J., Tank, J. L., Hamilton, S. K., Wollheim, W. M., Hall, R. O. Jr., Mulholland, P. J., Peterson, B. J., Ashkenas, L. R., Cooper, L. W., Dahm, C. N., Dodds, W. K., Grimm, N. B., Johnson, S. L., Mcdowell, W. H., Poole, G. C., Valett, H. M., Arango, C. P., Bernot, M. J., Burgim, A. J., Crenshaw, C. L., Helton, A. M., Johnson, L. T., O'Brien, J. M., Potter, J. D., Sheibley, R. W., Sobota, D. J., & Thomas, S. M. (2011). Nitrous oxide emission from denitrification in stream and river networks. Proceedings of the National Academy of Sciences, 108, 214– 219. https://doi.org/10.1073/pnas.1011464108

Borges, A. V., Darchambeau, F., Lambert, T., Bouillon, S., Morana, C., Brouyère, S., Hakoun, V., Jurado, A., Tseng, H. -C., Descy, J. -P., & Roland, F. A. E. (2018). Effects of agricultural land use on fluvial carbon dioxide, methane and nitrous oxide concentrations in a large European river, the Meuse (Belgium). Science of the Total Environment, 610-611, 342–355. https://doi.org/10.1016/j.scitotenv.2017.08.047

Butterbach-Bahl, K., Baggs, E. M., Dannenmann, M., Kiese, R., & Zechmeister-Boltenstern, S. (2013). Nitrous oxide emissions from soils: How well do we understand the processes and their controls? Philosophical Transactions of the Royal Society, B: Biological Sciences, 368(1621), 20130122–20130122. https://doi.org/10.1098/rstb.2013.0122

Chen, Y., Dong, S. L., Wang, F., Gao, Q. F., & Tian, X. L. (2016). Carbon dioxide and methane fluxes from feeding and no-feeding mariculture ponds. Environmental Pollution, 212, 489– 497. https://doi.org/10.1016/j.envpol.2016.02.039

Cheng, F., Zhang, H. M., Zhang, G. L., Liu, S. M., Song, G. D., & Du, G. X. (2019). Distribution and emission of N_2O in the largest river-reservoir system along the Yellow River. Science of the Total Environment, 666, 1209– 1219. https://doi.org/10.1016/j.scitotenv.2019.02.277

Cohen, Y., & Gordon, L. I. (1978). Nitrous oxide in the oxygen minimum of the eastern tropical North Pacific: Evidence for its consumption during denitrification and possible mechanisms for its production. Deep Sea Research: Part II, 25(6), 509– 524. https://doi.org/10.1016/0146-6291(78)90640-9

Cole, J. J., & Caraco, N. F. (1998). Atmospheric exchange of carbon dioxide in a low-wind oligotrophic lake measured by the addition of SF6. Limnology and Oceanography, 43(4), 647– 656. https://doi.org/10.4319/lo.1998.43.4.0647

Crosswell, J. R., Wetz, M. S., Hales, B., & Paerl, H. W. (2014). Extensive CO_2 emissions from shallow coastal waters during passage of Hurricane Irene (August 2011) over the Mid-Atlantic Coast of the U.S.A. Limnology and Oceanography, 59(5), 1651– 1665. https://doi.org/10.4319/lo.2014.59.5.1651

Dalsgaard, T., Stewart, F. J., Thamdrup, B., Brabandere, L. D., Revsbech, N. P., Ulloa, O., Canfield, D. E., & DeLon, E. F. (2014). Oxygen at nanomolar levels reversibly suppresses process rates and gene expression in anammox and denitrification in the oxygen minimum zone off northern Chile. mBio, 5(6), e01966-14. https://doi.org/10.1128/mBio.01966-14

Descloux, S., Chanudet, V., Serça, D., & Guérin, F. (2017). Methane and nitrous oxide annual emissions from an old eutrophic temperate reservoir. Science of the Total Environment, 598, 959– 972. https://doi.org/10.1016/j.scitotenv.2017.04.066

Ferrón, S., Ortega, T., Gómez-Parra, A., & Forja, J. M. (2007). Seasonal study of dissolved CH_4, CO_2 and N_2O in a shallow tidal system of the bay of Cádiz (SW Spain). Journal of Marine Systems, 66(1-4), 244– 257. https://doi.org/10.1016/j.jmarsys.2006.03.021

Food and Agriculture Organization (FAO). (2017). Fishery and aquaculture statistics (global aquaculture production 1950–2014). FishStatJ. http://www.fao.org/fishery/statistics/software/fishstatj/en

Goreau, T. J., Kaplan, W. A., Wofsy, S. C., McElroy, M. B., Valois, F. W., & Watson, S. W. (1980). Production of NO_2^- and N_2O by nitrifying bacteria at reduced concentrations of oxygen. Applied and Environmental Microbiology, 40(3), 526– 532. https://doi.org/10.1128/AEM.40.3.526-532.1980

Gruber, N., & Galloway, J. N. (2008). An Earth-system view of the global nitrogen cycle. Nature, 451(7176), 293– 296. https://doi.org/10.1038/nature06592

Gu, Y. G., Ouyang, J., Ning, J. J., & Wang, Z. H. (2017). Distribution and sources of organic carbon, nitrogen and their isotopes in surface sediments from the largest mariculture zone of the eastern Guangdong coast, South China. Marine Pollution Bulletin, 120(1-2), 286– 291. https://doi.org/10.1016/j.marpolbul.2017.05.013

Guérin, F., Abril, G., Tremblay, A., & Delmas, R. (2008). Nitrous oxide emissions from tropical hydroelectric reservoirs. Geophysical Research Letters, 35, L06404. https://doi.org/10.1029/2007GL033057

Hinshaw, S. E., & Dahlgren, R. A. (2013). Dissolved nitrous oxide concentrations and fluxes from the eutrophic San Joaquin River, California. Environmental Science & Technology, 47(3), 1313– 1322. https://doi.org/10.1021/es301373h

Hirota, M., Senga, Y., Seike, Y., Nohara, S., & Kunii, H. (2007). Fluxes of carbon dioxide, methane and nitrous oxide in two contrastive fringing zones of coastal lagoon, Lake Nakaumi, Japan. Chemosphere, 68(3), 597– 603. https://doi.org/10.1016/j.chemosphere.2007.01.002

Hu, B. B., Wang, D. Q., Zhou, J., Meng, W. Q., Li, C. W., Sun, Z. B., Guo, X., & Wang, Z. L. (2018). Greenhouse gases emission from the sewage draining rivers. Science of the Total Environment, 612, 1454– 1462. https://doi.org/10.1016/j.scitotenv.2017.08.055

Hu, Z., Lee, J. W., Chandran, K., Kim, S., & Khanal, S. K. (2012). Nitrous oxide (N$_2$O) emission from aquaculture: A review. Environmental Science & Technology, 46(12), 6470– 6480. https://doi.org/10.1016/10.1021/es300110x

Hu, Z., Lee, J. W., Chandran, K., Kim, S., Sharma, K., Brotto, A. C., & Khanal, S. K. (2013). Nitrogen transformations in intensive aquaculture system and its implication to climate change through nitrous oxide emission. Bioresource Technology, 130, 314– 320. https://doi.org/10.1016/j.biortech.2012.12.033

Hu, Z., Lee, J. W., Chandran, K., Kim, S., Sharma, K., & Khanal, S. K. (2014). Influence of carbohydrate addition on nitrogen transformations and greenhouse gas emissions of intensive aquaculture system. Science of the Total Environment, 470-471, 193– 200. https://doi.org/10.1016/j.scitotenv.2013.09.050

Intergovernmental Panel on Climate Change (IPCC) (2013). Climate change 2013: The physical science basis, Contribution of Working Group I to the Fifth Assessment Report of the Intergovernmental Panel on Climate Change. Cambridge: Cambridge University Press.

Jahne, B., Munnich, K. O., Bosinger, R., Dutzi, A., Huber, W., & Libner, P. (1987). On parameters influencing air-water exchange. Journal of Geophysical Research: Oceans, 92(C2), 1937– 1949. https://doi.org/10.1029/jc092ic02p01937

Ji, Q., Babbin, A. R., Jayakumar, A., Oleynik, S., & Ward, B. B. (2015). Nitrous oxide production by nitrification and denitrification in the eastern tropical South Pacific oxygen minimum zone. Geophysical Research Letters, 42, 10,755– 10,764. https://doi.org/10.1002/2015GL066853

Laini, A., Bartoli, M., Castaldi, S., Viaroli, P., Capri, E., & Trevisan, M. (2011). Greenhouse gases (CO$_2$, CH$_4$ and N$_2$O) in lowland springs within an agricultural impacted watershed (Po River Plain, northern Italy). Chemistry and Ecology, 27(2), 177– 187. https://doi.org/10.1080/02757540.2010.547489

Lévy, M., Lengaigne, M., Bopp, L., Vincent, E. M., Madec, G., Ethé, C., Kumar, D., & Sarma, V. V. S. S. (2012). Contribution of tropical cyclones to the air-sea CO$_2$ flux: A global view. Global Biogeochemical Cycles, 26, GB2001. https://doi.org/10.1029/2011GB004145

Li, F. F., Feng, J. F., Zhou, X. Y., Xu, C. C., Jijakli, M. H., Zhang, W. J., & Fang, F. P. (2019). Impact of rice-fish/shrimp co-culture on the N$_2$O emission and NH$_3$ volatilization in intensive aquaculture ponds. Science of the Total Environment, 655, 284– 291. https://doi.org/10.1016/j.scitotenv.2018.10.440

Liang, X., Xing, T., Li, J. X., Wang, B. L., Wang, F. S., He, C. Q., Hou, L. J., & Li, S. L. (2019). Control of the hydraulic load on nitrous oxide emissions from cascade reservoirs. Environmental Science & Technology, 53(20), 11745– 11754. https://doi.org/10.1021/acs.est.9b03438

Liu, S., Lin, F., & Wu, S. (2017). A meta-analysis of fertilizer-induced soil NO and combined NO+N_2O emissions. Global Change Biology, 23(6), 2520– 2532. https://doi.org/10.1111/gcb.13485

Liu, S. W., Hu, Z. Q., Wu, S., Li, S. Q., Li, Z. F., & Zou, J. W. (2016). Methane and nitrous oxide emissions reduced following conversion of rice paddies to inland crab-fish aquaculture in southeast China. Environmental Science & Technology, 50(2), 633– 642. https://doi.org/10.1021/acs.est.5b04343

Liu, Y. S., Zhu, R. B., Ma, D. W., Xu, H., Luo, Y. H., Huang, T., & Sun, L. G. (2011). Temporal and spatial variations of nitrous oxide fluxes from the littoral zones of three alga-rich lakes in coastal Antarctica. Atmospheric Environment, 45(7), 1464– 1475. https://doi.org/10.1016/j.atmosenv.2010.12.017

Ma, Y. C., Sun, L. Y., Liu, C. Y., Yang, X. Y., Zhou, W., Yang, B., Schwenke, G., & Liu, D. L. (2018). A comparison of methane and nitrous oxide emissions from inland mixed-fish and crab aquaculture ponds. Science of the Total Environment, 637-638, 517– 523. https://doi.org/10.1016/j.scitotenv.2018.05.040

Maavara, T., Lauerwald, R., Laruelle, G. G., Akbarzadeh, Z., Bouskill, N. J., Van Cappellen, P., & Regnier, P. (2019). Nitrous oxide emissions from inland waters: Are IPCC estimates too high? Global Change Biology, 25(2), 473– 488. https://doi.org/10.1111/gcb.14504

MacIntyre, S., Wanninkhof, R., & Chanton, J. P. (1995). Trace gas exchange across the air-water interface in freshwater and coastal marine environment. In P. A. Matson, & R. C. Harriss (Eds.), Biogenic trace gases: Measuring emission from soil and water (pp. 52– 97). Cambridge: Blackwell Scientific Publications Ltd.

Massara, T. M., Malamis, S., Guisasola, A., Baeza, J. A., Noutsopoulos, C., & Katsou, E. (2018). A review on nitrous oxide (N_2O) emissions during biological nutrient removal from municipal wastewater and sludge reject water. Science of the Total Environment, 596-597, 106– 123. https://doi.org/10.1016/j.scitotenv.2017.03.191

McCarl, B. A., & Schneider, U. A. (2001). Greenhouse gas mitigation in U.S. agriculture and forestry. Science, 94(2), 128– 140. https://doi.org/10.1016/j.agsy.2006.08.001

Murray, R. H., Erler, D. V., & Eyre, B. D. (2015). Nitrous oxide fluxes in estuarine environments: Response to global change. Global Change Biology, 21(9), 3219– 3245. https://doi.org/10.1111/gcb.12923

Musenze, R. S., Grinham, A., Werner, U., Gale, D., Sturm, K., Udy, J., & Yuan, Z. G. (2014). Assessing the spatial and temporal variability of diffusive methane and nitrous oxide emissions from subtropical freshwater reservoirs. Environmental Science & Technology, 48(24), 14499– 14507. https://doi.org/10.1021/es505324h

Natchimuthu, S., Sundgren, I., Gålfalk, M., Klemedtsson, L., & Bastviken, D. (2017). Spatiotemporal variability of lake pCO_2 and CO_2 fluxes in a hemiboreal catchment. Journal of Geophysical Research: Biogeosciences, 122, 30– 49. https://doi.org/10.1002/2016JG003449

Natchimuthu, S., Sundgren, I., Gålfalk, M., Klemedtsson, L., Crill, P., Danielsson, Å., & Bastviken, D. (2016). Spatio-temporal variability of lake CH_4 fluxes and its influence on annual whole lake emission estimates. Limnology and Oceanography, 61(S1), S13– S26. https://doi.org/10.1002/lno.10222

Nemoto, K., Midorikawa, T., Wada, A., Ogawa, K., Takatani, S., Kimoto, H., Ishii, M., & Inoue, H. Y. (2009). Continuous observations of atmospheric and oceanic CO_2 using a moored buoy in the East China Sea: Variations during the passage of typhoons. Deep Sea Research Part II: Topical Studies in Oceanography, 56(8-10), 542– 553. https://doi.org/10.1016/j.dsr2.2008.12.015

Paudel, S. R., Choi, O., Khanal, S. K., Chandran, K., Kim, S., & Lee, J. W. (2015). Effects of temperature on nitrous oxide (N_2O) emission from intensive aquaculture system. Science of the Total Environment, 518-519, 16– 23. https://doi.org/10.1016/j.scitotenv.2015.02.076

Rajkumar, A. N., Barnes, J., Ramesh, R., Purvaja, R., & Upstill-Goddard, R. C. (2008). Methane and nitrous oxide fluxes in the polluted Adyar River and estuary, SE India. Marine Pollution Bulletin, 56(12), 2043– 2051. https://doi.org/10.1016/j.marpolbul.2008.08.005

Ravishankara, A. R., Daniel, J. S., & Portmann, R. W. (2009). Nitrous oxide (N_2O): The dominant ozone-depleting substance emitted in the 21st century. Science, 326(5949), 123– 125. https://doi.org/10.1126/science.1176985

Rosamond, M. S., Thuss, S. J., & Schiff, S. L. (2012). Dependence of riverine nitrous oxide emissions on dissolved oxygen levels. Nature Geoscience, 5(10), 715– 718. https://doi.org/10.1038/ngeo1556

Rosamond, M. S., Thuss, S. J., Schiff, S. L., & Elgood, R. J. (2011). Coupled cycles of dissolved oxygen and nitrous oxide in rivers along a trophic gradient in Southern Ontario, Canada. Journal of Environment Quality, 40(1), 256– 270. https://doi.org/10.2134/jeq2010.0009

Silvennoinen, H., Liikanen, A., Torssonen, J., Stange, C. F., & Martikainen, P. J. (2008). Denitrification and nitrous oxide effluxes in boreal, eutrophic river sediments under increasing nitrate load: A laboratory microcosm study. Biogeochemistry, 91(2-3), 105– 116. https://doi.org/10.2307/40343622

Sturm, K., Yuan, Z., Gibbes, B., Werner, U., & Grinham, A. (2014). Methane and nitrous oxide sources and emissions in a subtropical freshwater reservoir, South East Queensland, Australia. Biogeosciences, 11(18), 5245– 5258. https://doi.org/10.5194/bg-11-5245-2014

Sutka, R. L., Ostrom, N. E., Ostrom, P. H., Breznak, J. A., Gandhi, H., Pitt, A. J., & Li, F. (2006). Distinguishing nitrous oxide production from nitrification and denitrification on the basis of isotopomer abundances. Appl. Environ. Microb., 72(1), 638– 644. https://doi.org/10.1128/aem.72.1.638-644.2006

Tan, Y. J. (2014). The greenhouse gases emission and production mechanism from river sediment in Shanghai. Shanghai: East China Normal University. (in Chinese)

Tong, C., Wang, W. Q., Zeng, C. S., & Marrs, R. (2010). Methane emissions from a tidal marsh in the Min River estuary, southeast China. Journal of Environmental Science and Health Part A, 45(4), 506– 516. https://doi.org/10.1080/10934520903542261

Verdegem, M. C. J., & Bosma, R. H. (2009). Water withdrawal for brackish and inland aquaculture, and options to produce more fish in ponds with present water use. Water Policy, 11(Suppl 1), 52– 68. https://doi.org/10.2166/wp.2009.003

Wang, D. Q., Tan, Y. J., Yu, Z. J., Li, Y. J., Chang, S. Q., Deng, H. H., Hu, B. B., & Chen, Z. L. (2015). Nitrous oxide production in river sediment of highly urbanized Aarea and the effects of water quality. Wetlands, 35(6), 1213– 1223. https://doi.org/10.1007/s13157-015-0708-5

Wang, H. J., Wanga, W. D., Yin, C. Q., Wang, Y. C., & Lu, J. W. (2006). Littoral zones as the "hotspots" of nitrous oxide (N_2O) emission in a hyper-eutrophic lake in China. Atmospheric Environment, 40(28), 5522– 5527. https://doi.org/10.1016/j.atmosenv.2006.05.032

Wang, H. X., Zhang, L., Yao, X. L., Xue, B., & Yan, W. J. (2017). Dissolved nitrous oxide and emission relating to denitrification across the Poyang Lake aquatic continuum. Journal of Environmental Sciences, 52, 130– 140. https://doi.org/10.1016/j.jes.2016.03.021

Wang, J. N., Chen, N. W., Yan, W. J., Wang, B., & Yang, L. B. (2015). Effect of dissolved oxygen and nitrogen on emission of N_2O from rivers in China. Atmospheric Environment, 103, 347– 356. https://doi.org/10.1016/j.atmosenv.2014.12.054

Wang, S. L., Liu, C. Q., Yeager, K. M., Wan, G. J., Li, J., Tao, F. X., Lü, Y. C., Liu, F., & Fan, C. X. (2009). The spatial distribution and emission of nitrous oxide (N_2O) in a large eutrophic lake in eastern China: Anthropogenic effects. Science of the Total Environment, 407(10), 3330– 3337. https://doi.org/10.1016/j.scitotenv.2008.10.037

Wang, X. F., He, Y. X., Yuan, X. Z., Chen, H., Peng, C. H., Yue, J. S., Zhang, Q. Y., Diao, Y. B., & Liu, S. S. (2017). Greenhouse gases concentrations and fluxes from subtropical small reservoirs in relation with watershed urbanization. Atmospheric Environment, 154, 225– 235. https://doi.org/10.1016/j.atmosenv.2017.01.047

Wang, X. M., Hu, M. J., Ren, H. C., Li, J. B., Tong, C., & Musenze, R. S. (2018). Seasonal variations of nitrous oxide fluxes and soil denitrification rates in subtropical freshwater and brackish tidal marshes of the Min River estuary. Science of the Total Environment, 616-617, 1404– 1413. https://doi.org/10.1016/j.scitotenv.2017.10.175

Wenk, C. B., Frame, C. H., Koba, K., Casciotti, K. L., Veronesi, M., Niemann, H., Schubert, C. J., Yoshida, N., Toyoda, S., Makabe, A., Zopfi, J., & Lehmann, M. F. (2016). Differential N_2O dynamics in two oxygendeficient lake basins revealed by stable isotope and isotopomer distributions. Limnology and Oceanography, 61(5), 1735– 1749. https://doi.org/10.1002/lno.10329

Whitfield, C. J., Aherne, J., & Baulch, H. M. (2011). Controls on greenhouse gas concentrations in polymictic headwater lakes in Ireland. Science of the Total Environment, 410-411, 217– 225. https://doi.org/10.1016/j.scitotenv.2011.09.045

Williams, J., & Crutzen, P. J. (2010). Nitrous oxide from aquaculture. Nature Geoscience, 3(3), 143. https://doi.org/10.1038/ngeo804

World Meteorological Organization (WMO). (2019). WMO Greenhouse Gas Bulletin No. 15 (25 November 2019). https://library.wmo.int/doc_num.php?explnum_id=5455.pdf

Wu, S., Hu, Z. Q., Hu, T., Chen, J., Yu, K., Zou, J. W., & Liu, S. W. (2018). Annual methane and nitrous oxide emissions from rice paddies and inland fish aquaculture wetlands in

southeast China. Atmospheric Environment, 175, 135– 144.
https://doi.org/10.1016/j.atmosenv.2017.12.008

Xia, X. H., Zhang, S. B., Li, S. L., Zhang, L. W., Wang, G. Q., Zhang, L., Wang, J. F., & Li, Z. H. (2018). The cycle of nitrogen in river systems: Sources, transformation, and flux. Environmental Science: Processes & Impacts, 20(6), 863– 891. https://doi.org/10.1039/C8EM00042E

Xiao, Q. T., Xu, X. F., Zhang, M., Duan, H. T., Hu, Z. H., Wang, W., Xiao, W., & Lee, X. H. (2019). Coregulation of nitrous oxide emissions by nitrogen and temperature in China's third largest freshwater Lake (Lake Taihu). Limnology and Oceanography, 64(3), 1070– 1086. https://doi.org/10.1002/lno.11098

Xiao, Q. T., Zhang, M., Hu, Z. H., Gao, Y. Q., Hu, C., Liu, C., Liu, S. D., Zhang, Z., Zhao, J. Y., Xiao, W., & Lee, X. (2017). Spatial variations of methane emission in a large shallow eutrophic lake in subtropical climate. Journal of Geophysical Research: Biogeosciences, 122, 1597– 1614. https://doi.org/10.1002/2017JG003805

Xing, Y. P., Xie, P., Yang, H., Ni, L. Y., Wang, Y. S., & Tang, W. H. (2004). Diel variation of methane fluxes in summer in a eutrophic subtropical lake in China. Journal of Freshwater Ecology, 19(4), 639– 644. https://doi.org/10.1080/02705060.2004.9664745

Yang, H., & Flower, R. J. (2012). Potentially massive greenhouse-gas sources in proposed tropical dams. Frontiers in Ecology and the Environment, 10(5), 234– 235. https://doi.org/10.2307/41811805

Yang, H., Xie, P., Ni, L., & Flower, R. J. (2011). Underestimation of CH_4 emission from freshwater lakes in China. Environmental Science & Technology, 45(10), 4203– 4204. https://doi.org/10.1021/es2010336

Yang, P., Bastviken, D., Jin, B. S., Mou, X. J., & Tong, C. (2017). Effects of coastal marsh conversion to shrimp aquaculture ponds on CH_4 and N_2O emissions. Estuarine, Coastal and Shelf Science, 199, 125– 131. https://doi.org/10.1016/j.ecss.2017.09.023

Yang, P., Lai, D. Y. F., Jin, B. S., Bastviken, D., Tan, L. S., & Tong, C. (2017). Dynamics of dissolved nutrients in the aquaculture shrimp ponds of the Min River estuary, China: Concentrations, fluxes and environmental loads. Science of the Total Environment, 603-604, 256– 267. https://doi.org/10.1016/j.scitotenv.2017.06.074

Yang, P., Zhang, Y., Yang, H., Zhang, Y. F., Xu, J., Tan, L. S., Tong, C., & Lai, D. Y. F. (2019). Large fine-scale spatiotemporal variations of CH_4 diffusive fluxes from shrimp

aquaculture ponds affected by organic matter supply and aeration in Southeast China. Journal of Geophysical Research: Biogeosciences, 124, 1290– 1307. https://doi.org/10.1029/2019JG005025

Yang, P., Zhang, Y. F., Lai, D. Y. F., Tan, L. S., Jin, B. S., & Tong, C. (2018). Fluxes of carbon dioxide and methane across the water–atmosphere interface of aquaculture shrimp ponds in two subtropical estuaries: The effect of temperature, substrate, salinity and nitrate. Science of the Total Environment, 635, 1025– 1035. https://doi.org/10.1016/j.scitotenv.2018.04.102

Ye, H. J., Sheng, J. Y., Tang, D. L., Siswanto, E., Kalhoro, M. A., & Sui, Y. (2017). Storm-induced changes in pCO_2 at the sea surface over the northern South China Sea during Typhoon Wutip. Journal of Geophysical Research: Oceans, 122, 4761– 4778. https://doi.org/10.1002/2016JC012643

Yogev, U., Atari, A., & Gross, A. (2018). Nitrous oxide emissions from near-zero water exchange brackish recirculating aquaculture systems. Science of the Total Environment, 628-629, 603– 610. https://doi.org/10.1016/j.scitotenv.2018.02.089

Yu, Z. J., Deng, H. G., Wang, D. Q., Ye, M. W., Tan, Y. J., Li, Y. J., Chen, Z. L., & Xu, S. Y. (2013). Nitrous oxide emissions in the shanghai river network: Implications for the effects of urban sewage and IPCC methodology. Global Change Biology, 19(10), 2999– 3010. https://doi.org/10.1111/gcb.12290

Yu, J. H., Zhang, J. Y., Chen, Q. W., Yu, W. Y., Hu, L. M., Shi, W. Q., Zhong, J. C., & Yan, W. X. (2018). Dramatic source-sink transition of N_2O in the water level fluctuation zone of the Three Gorges Reservoir during flooding-drying processes. Environmental Science and Pollution Research, 25, 20,023– 20,031. https://doi.org/10.1007/s11356-018-2190-0

Zhang, Y. F., Yang, P., Yang, H., Tan, L. S., Guo, Q. Q., Zhao, G. H., Li, L., Gao, Y. C., & Tong, C. (2019). Plot-scale spatiotemporal variations of CO_2 concentration and flux across water-air interfaces at aquaculture shrimp ponds in a subtropical estuary. Environmental Science and Pollution Research, 26(6), 5623– 5637. https://doi.org/10.1007/s11356-018-3929-3

Table 1. Comparison of N$_2$O Concentrations (nmol L^{-1}>) and Diffusive Flux (nmol m^{-2} hr^{-1}) Across the Water-Air Interface in Mariculture Ponds, Reservoirs, Lakes, and Rivers

Ecosystems type	Study site	Study period	N$_2$O concentration	N$_2$O flux	Reference
Aquaculture pond	Min River Estuary, China	June to November 2017	4.2 to 23.1 (9.5)	0.2 to 948.3 (169.1)[a]	Present study
	Jiangsu Province, China	November 2013 to November 2014	—	48.80[b]	S. W. Liu et al. (2016)
	Choongnam Province, Vietnam	—	—	46.9 to 76.9 (—)	Paudel et al. (2015)
	Zhejiang Province, China	August 2016 to July 2017	—	−35.8 to 48.5 (—)[b]	Li et al. (2019)
	Jiangsu Province, China	January 2014 to January 2015	—	55.58[b]	Wu et al. (2018)
Reservoir	Southeast Queensland, Australia	August and November 2011 and February and May 2012	—	−3.4 to 80.3 (9.2)[a]	Musenze et al. (2014)
	Eguzon Reservoir, France	January to December 2011	10 to 1,460	112.5 to 3229.2 (716.7)[a]	Descloux et al. (2017)
	Three Gorges Reservoir, China	June 2017	—	−14.58 to 117.5 (—)[a]	Yu et al. (2018)
	Chongqing, Southwest China	September 2014 to June 2015	12 to 379 (90)	83.3 to 277.5 (5,458.3)[a]	H. X. Wang, Zhang, et al. (2017)
	Petit Saut Reservoir, French Guiana and Fortuna Reservoir, Panama	May and December 2003	—	−5,625 to 9,128 (3,800)[b]	Guérin et al. (2008)
Lake	Poyang Lake, China	July to August 2013	90 to 1,050	−9.2 to 120.3 (16.6)[b]	X. F. Wang, He, et al. (2017)
	Taihu Lake, China	August 2003 to August 2004	—	−2,821 to 2132.1 (435.8)[b]	H. J. Wang et al. (2006)
	Lakes Mochou, Tuanjie, Daming, Antarctica	Summers of 2007/2008 and 2008/2009	—	2.5 to 7.3 (4.3)[b]	Y. S. Liu et al. (2011)
	Lake Nakaumi, Japan	Midsummer 2003	—	20.3 to 50.7 (30.4)[b]	Hirota et al. (2007)
River	Springs in the Po River watershed, Italy	Summer 2009	20 to 1,020 (370)	71,022.7 to 121,753.3 (113,636.4)[a]	Laini et al. (2011)
	Drainage rivers in Tianjin	July and October 2014 and January and April 2015	30 to 80 (50)	460.2 to 3,771.4 (1,860.3)[a]	B. Hu et al. (2018)
	Rivers in Shanghai	December 2011 to October 2012	10 to 1,070 (110)	20.0 to 21,310.0 (2,865.0)[a]	Tan (2014)
	Temmesjoki River, Finland	May 2003	—	435.6 to 2,746.2 (—)[a]	Silvennoinen et al. (2008)
	Adyar River, India	August 2003 to December 2004	4 to 450	10.0 to 5,100.0[a]	Rajkumar et al. (2008)
	Río San Pedro Creek, Spain	February, May, July, and September 2004	10 to 50	1,000.0 to 2,583.3[a]	Ferrón et al. (2007)

Note. Numbers in brackets are averages. "—" indicated no data.

[a] N$_2$O fluxes were measured by gas transfer equation method.

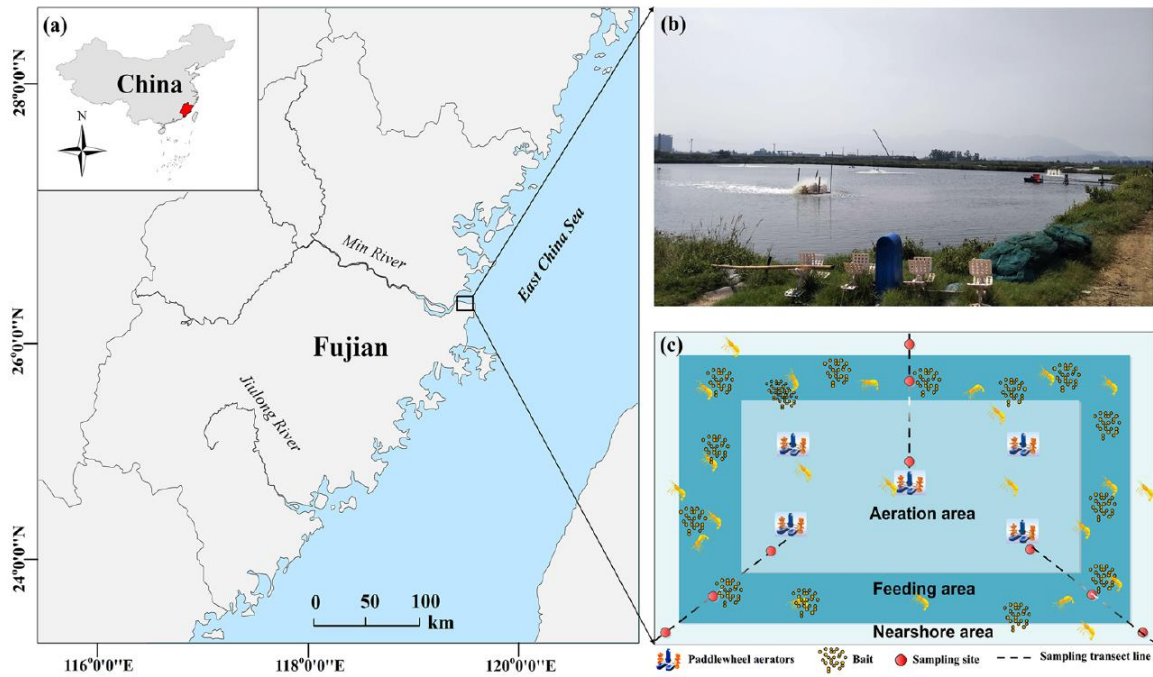[b] N$_2$O fluxes were measured by a closed chamber technique.

Figure 1. (a) Location of the study area at Shanyutan Wetland of Min River Estuary, Southeast China, (b) a photo showing one of the studied ponds, and (c) a diagram showing the locations of sampling sites (red dots) within the pond. Zones N, F, and A are nearshore, feeding, and aeration areas, respectively (modified after P. Yang et al., 2019).
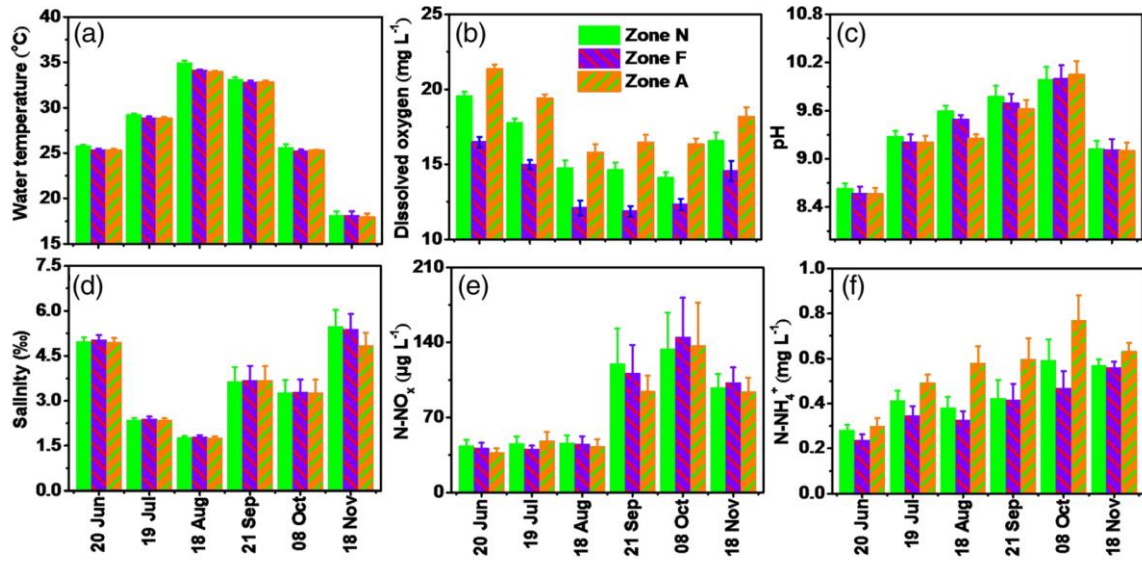
Figure 2. (a–f) Variations of environmental factors among the three zones in the mariculture ponds during the aquaculture period. Zones N, F, and A are nearshore, feeding, and aeration areas, respectively. The bars represent the means ±1 standard error ($n = 9$).
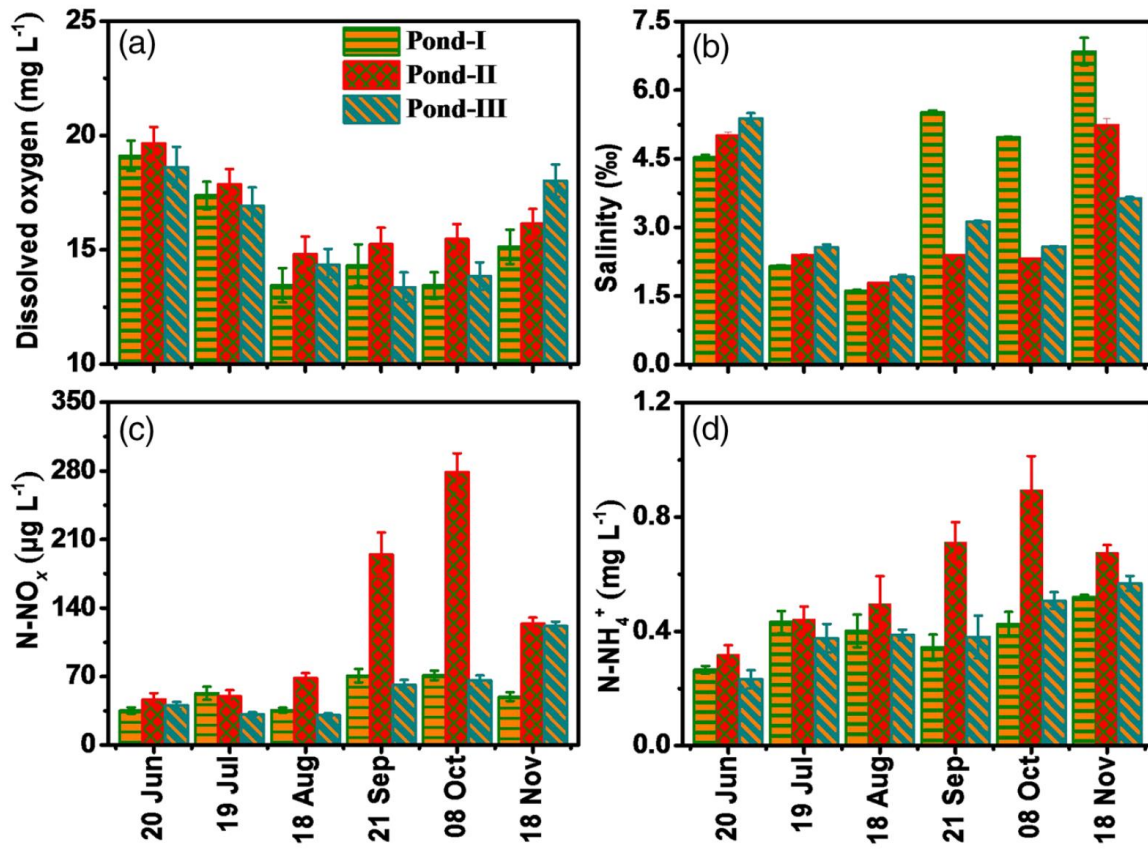
Figure 3. (a–d) Variations of environmental factors among the three mariculture ponds during the aquaculture period. The bars represent the means ±1 standard error ($n = 9$).
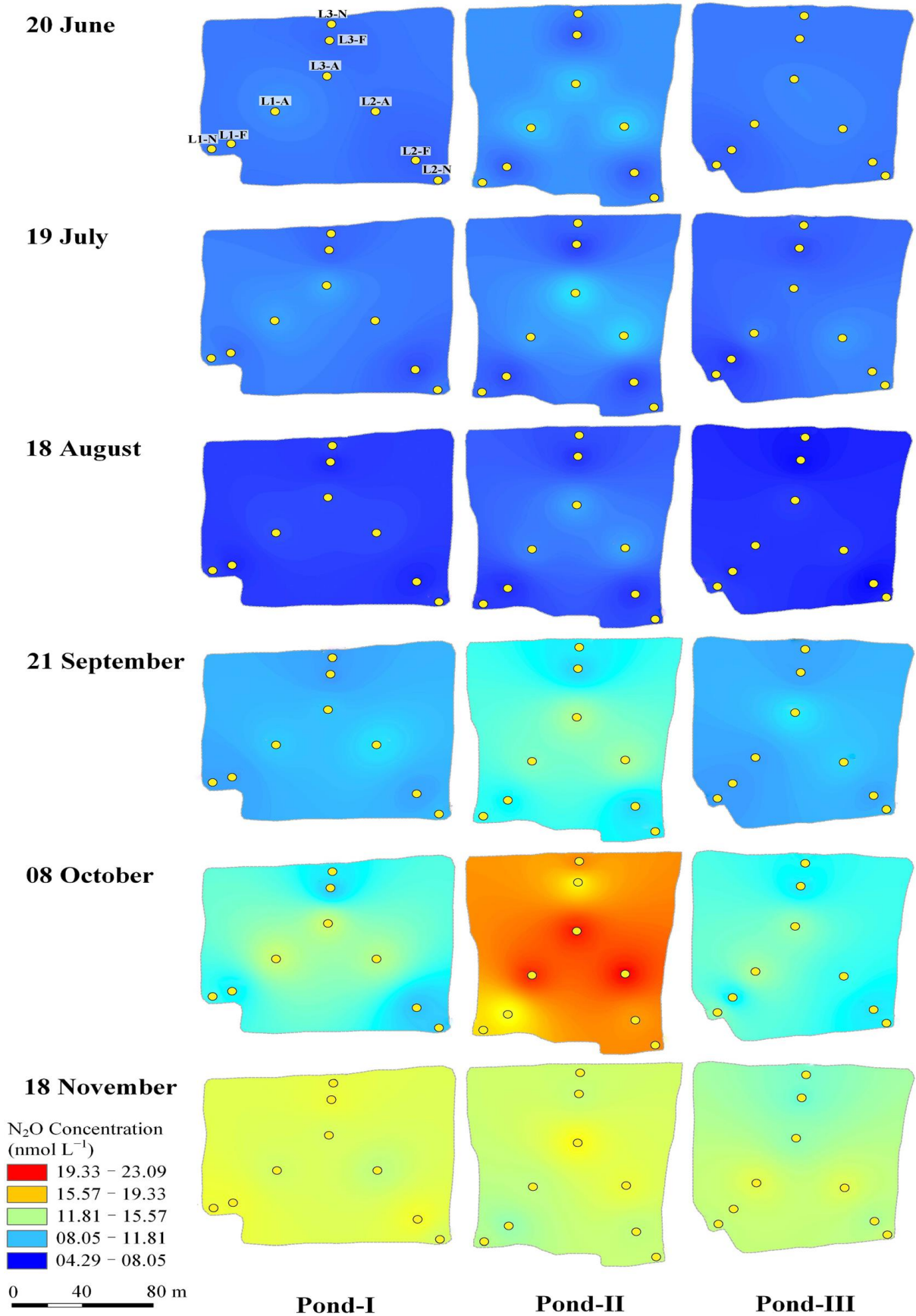
Figure 4. Within-pond variations of N$_2$O concentrations in the surface water (20-cm depth) of the three studied shrimp ponds during the aquaculture period.
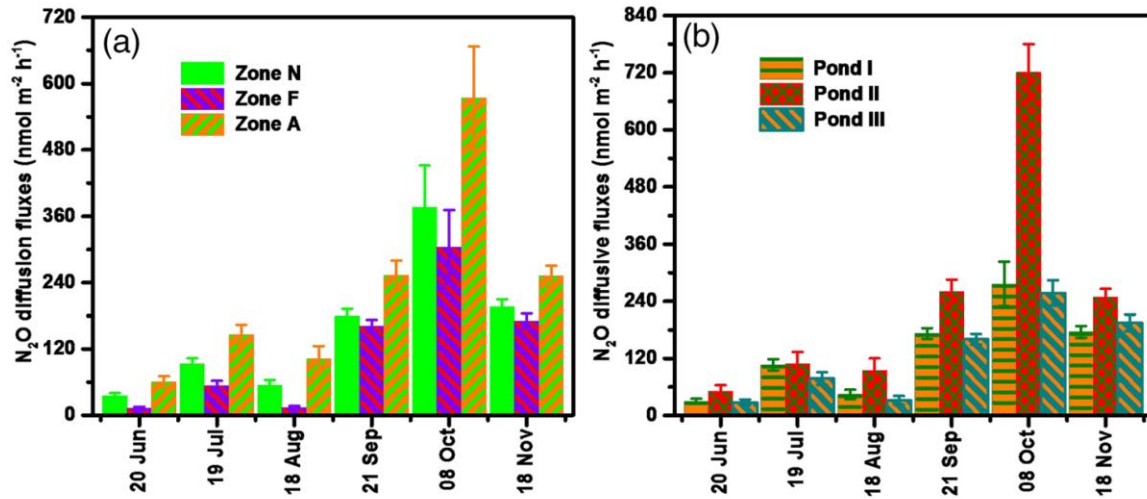
Figure 5. Spatial variations of N2O diffusive flux across the water-air interface of shrimp ponds during the aquaculture period, when averaged by (a) nearshore, feeding, and aeration zones, and (b) Ponds I, II, and III. The bars represent the means ±1 standard error (n ¼ 9). Zones N, F, and A are nearshore area, feeding area, and aeration area, respectively.